Contribution from the Laboratoire de Chimie-Physique
(UA 253 du CNRS), HEI, 59046 Lille Cédex, France

The Solubilization Process of Sulfur in Liquid Ammonia and the Equilibrium State of These Solutions

P. Dubois, J. P. Lelieur,* and G. Lepoutre

Received February 17, 1988

The UV–visible absorption spectrum has been monitored versus time at given temperatures (−35 and −15 °C) during the solubilization process of sulfur in liquid ammonia. These experiments allow the determination of the absorption spectrum at equilibrium. During the solubilization, the heptasulfur imido anion, S_7N^-, is not observed. The species S_3N^- goes through a maximum concentration, and S_3N^- is the precursor species of S_4N^-. The addition of ammonium chloride to ammonia slows down the first steps of the solubilization, while the opposite influence is found when alkali amide is added to ammonia. These observations are used to propose a model of the reaction mechanism between sulfur and ammonia. The equilibrium distribution of solubilized sulfur is quantitatively analyzed. At least 50% of solubilized sulfur is in the zero oxidation state, but not with the S_8 structure.

Introduction

The understanding of the solution of sulfur in liquid ammonia has been greatly improved by the unambiguous identification of S_4N^- and S_3^- in these solutions.[1-3] This identification was the proof that the solubilization of sulfur in ammonia is a redox disproportionation process. Chivers and Lau[1] proposed a reaction mechanism in which the first step is the nucleophilic attack of cyclic sulfur, *c*-S_8, by the amide ion NH_2^- resulting from the self-dissociation of ammonia. This nucleophilic attack produces $S_8NH_2^-$ that disproportionates, giving first S_7N^- and H_2S and subsequently S_4N^- and an ammonium polysulfide. Bernard et al. suggested that the equilibrium state of the solutions could be described by the equations[3]

$$10S + 4NH_3 \rightarrow S_4N^- + S_6^{2-} + 3NH_4^+ \quad (1)$$

$$S_6^{2-} \rightleftarrows 2S_3^- \quad (2)$$

It was shown[4] later that eq 1 is oversimplified because S_4N^- is not the only oxidized species detected spectroscopically when solutions have reached equilibrium. The influence of the addition of an alkali amide on the solutions was also investigated recently.[5] This study has shown that a large amount of solubilized sulfur is at the zero oxidation state when solutions have reached equilibrium. This is an important point not described by eq 1. The spectroscopic investigation of the solutions of lithium polysulfides in liquid ammonia[6] and of ammonium polysulfides in liquid ammonia[7] has shown that S_6^{2-} is the least reduced form of sulfur in liquid ammonia. The Raman spectral comparison of polysulfide solutions and of sulfur solutions shows that S_6^{2-} is the reduced form of sulfur resulting from the disproportionation of sulfur in liquid ammonia.

The experimental results given in this paper have been initiated by the publication[8-11] of absorption spectra of solutions of sulfur in liquid ammonia that display significant differences from those we have obtained. We had always observed that the absorption band at 580 nm is higher than that at ca. 450 nm, while the opposite result was displayed in other papers.[8-11] It was then suspected that some of these absorption spectra could have been obtained for solutions that were not in the equilibrium state. Consequently, it was decided to record the UV–visible absorption spectrum of the solutions during the solubilization process.

These experiments have been used to determine the concentrations of some chemical species during this process. This led us to analyze the reaction mechanism proposed by Chivers and Lau[1] and to propose a new one. Finally, an improved description of the equilibrium state of the solutions is given through a quantitative determination of the solubilized sulfur that is at the zero oxidation state at equilibrium.

Experimental Section

The samples for the study of the solubilization process with UV–visible spectrophotometry experiments have been prepared by the procedure previously described.[4,5] Sulfur (Fluka, >99.999%) was used without further purification. A weighed amount of sulfur was introduced into the cell, which was then pumped down to about 10^{-6} Torr for several hours. Dried ammonia was condensed onto sulfur at dry ice temperature in a quartz optical cell, which was then sealed off. The amount of ammonia was controlled by gas volumetry. Absorption spectra have been recorded at a given temperature with an Oxford Instruments DN 704 cryostat; the temperature of the sample was regulated within ±0.1 °C. Absorption spectra have been recorded at regular intervals on a Beckman 5240 UV–visible spectrophotometer. When the solubilization process was under study at −35 °C, the sample was always at this temperature, either in the optical cryostat or in an alcohol cryostat. When the solubilization process was under study at −15 °C, the sample was either at this temperature in the optical cryostat or at dry ice temperature. It is known and it was confirmed that the solubilization process is stopped at dry ice temperature. Consequently, for the study of the solubilization process at −15 °C, the amount of time taken into account was the time spent by the sample in the optical cryostat. Since it is known[2-4,8] that solutions of sulfur in liquid ammonia are photosensitive, the samples were always kept in the dark.

Results

The Equilibrium State. The experiments reported below show quantitatively that the solubilization process of sulfur in liquid ammonia is slow. With samples prepared for rather concentrated solutions (ca. 10^{-2} M), the equilibrium state is reached after about 1000 h at −35 °C (Figures 1 and 2), while it is reached after about 100 h at −15 °C (Figure 3). For a sample of the same composition kept at least 2 days at room temperature (in the dark), the absorption spectra at −35 and −15 °C cannot be distinguished from those obtained when the solubilization is fully performed either at −35 or at −15 °C. It was also verified that the absorption spectra at room temperature or below, for samples presumably in the equilibrium state, are not modified after the sample has been kept several hours at +50 °C. Our experiments show that the time required to reach equilibrium is strongly temperature dependent. These experiments have not been conducted for concentrations lower than 10^{-2} M and for temperatures below −35 °C, because it was observed that the solubilization is then extremely slow. Our experiments show that the absorption spectra reported[4,5] after solubilization at room temperature were indeed related to the equilibrium state.

In Figure 1, several absorption spectra recorded during the solubilization process at −35 °C are displayed. Spectrum d in Figure 1 was recorded after about 1000 h at −35 °C, and the solution was then in the equilibrium state. The variations of the absorbance at several wavelengths versus time are plotted in Figure 2 for another set of experimental values; this confirms the results displayed in Figure 1. It is shown in Figures 1 and 2 that the relative concentrations of chemical species are significantly

(1) Chivers, T.; Lau, C. *Inorg. Chem.* **1982**, *21*, 453.
(2) Bernard, L. Thèse de docteur ingênieur, Lille, 1982.
(3) Bernard, L.; Lelieur, J. P.; Lepoutre, G. *Nouv. J. Chim.* **1985**, *9*, 199.
(4) Dubois, P.; Lelieur, J. P.; Lepoutre, G. *Inorg. Chem.* **1987**, *26*, 1899.
(5) Dubois, P.; Lelieur, J. P.; Lepoutre, G. *Inorg. Chem.* **1988**, *27*, 3032.
(6) Dubois, P.; Lelieur, J. P.; Lepoutre, G. *Inorg. Chem.* **1988**, *27*, 73.
(7) Dubois, P.; Lelieur, J. P.; Lepoutre, G. *Inorg. Chem.* **1988**, *27*, 1883.
(8) Prestel, H.; Schindewolf, U. *Ber. Bunsen-Ges. Phys. Chem.* **1986**, *90*, 150.
(9) Prestel, H.; Seelert, S.; Schindewolf, U. *Z. Physik. Chem. (Munich)* **1986**, *148*, 97.
(10) Prestel, H. Ph.D. Dissertation, University of Karlsrühe, 1986.
(11) Prestel, H.; Schindewolf, U. *Z. Anorg. Allg. Chem.* **1987**, *551*, 21.

0020-1669/89/1328-0195$01.50/0

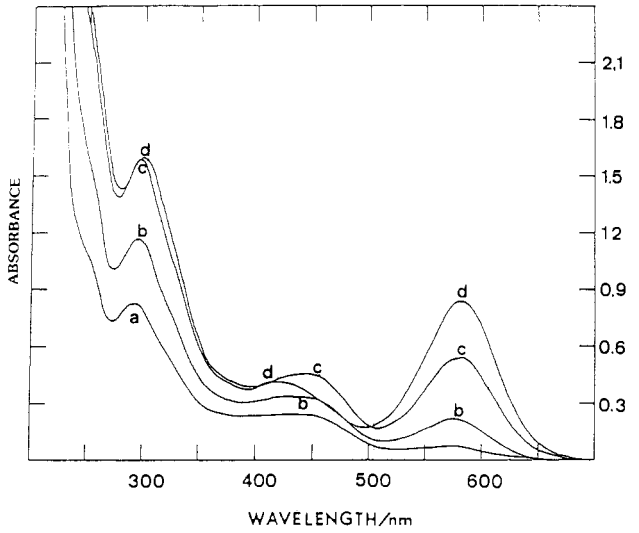

Figure 1. Absorption spectra at −35 °C of a sulfur–ammonia sample during the solubilization process at −35 °C: (a) 336 h after the beginning of the solubilization process; (b) after 528 h; (c) after 698 h; (d) after 1000 h. The concentration of the solution after completion of the solubilization is 1.5×10^{-2} M. Optical path length = 1 mm. Spectrum d corresponds to the equilibrium state of the solution.

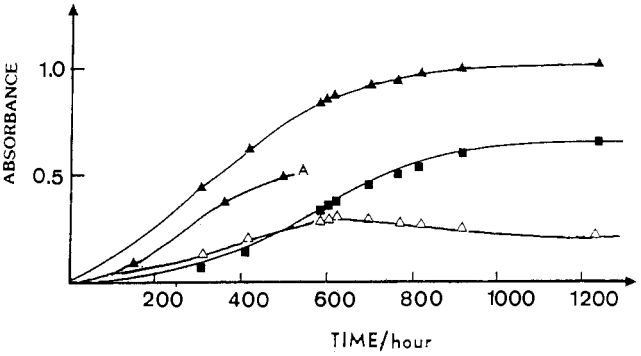

Figure 2. Variations of the absorbance at −35 °C versus time, at various wavelengths, during the solubilization process at −35 °C of a sulfur–ammonia sample: (▲) 300 nm; (△) 460 nm; (■) 580 nm. The concentration of the solution after completion of the solubilization is 1.1×10^{-2} M. Optical path length = 1 mm. Curve A displays the variations of absorbance at 300 nm under the same conditions, but with ammonium chloride addition (10^{-2} M); these variations are also displayed in Figure 6.

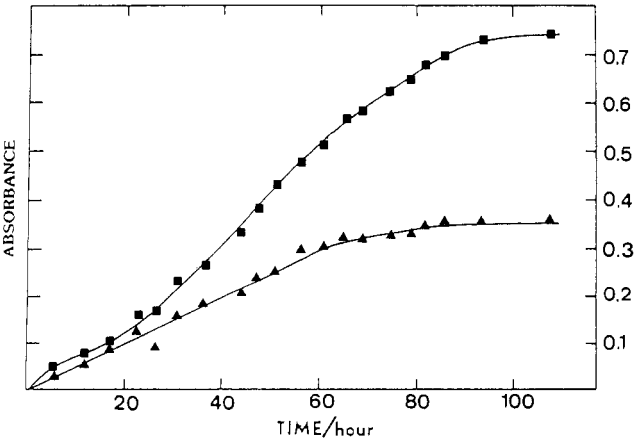

Figure 3. Variations of the absorbance at −15 °C versus time, at two wavelengths, during the solubilization process at −15 °C of a sulfur–ammonia sample: (▲) 420 nm; (■) 580 nm. The concentration of the solution after completion of the solubilization is 1.5×10^{-2} M. Optical path length = 1 mm.

changed during the solubilization process. This will be discussed below. It must be emphasized that the equilibrium state is not

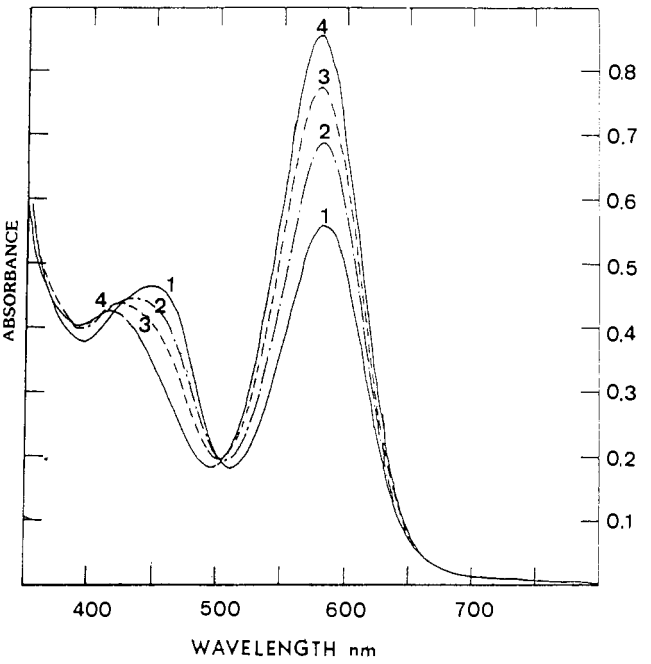

Figure 4. Absorption spectra at −35 °C obtained from the same sample and in the same conditions as those of Figure 1: (1) 696 h after the beginning of the solubilization; (2) after 744 h; (3) after 816 h; (4) after 830 h. These spectra have been obtained when solid sulfur is no longer visually detected in the sample. Optical path length = 1 mm.

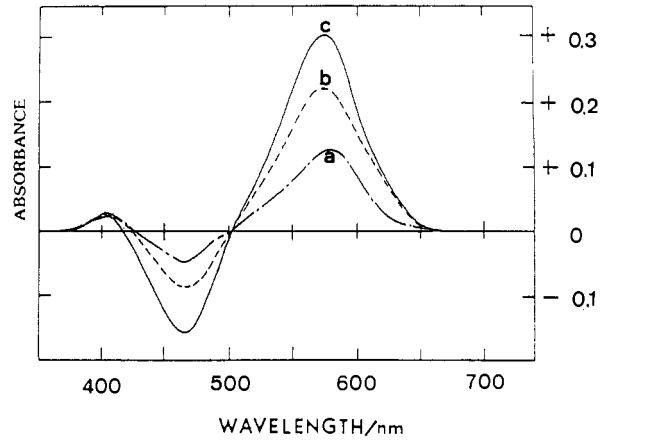

Figure 5. Differences between the spectra 2–4 of Figure 4 and spectrum 1 of Figure 4: (a) (2) − (1); (b) (3) − (1); (c) (4) − (1).

yet reached when solid sulfur has visually disappeared. For the sample associated with the results displayed in Figure 1, solid sulfur was no longer visually detected after about 700 h at −35 °C, and spectrum c was then recorded; it is seen that spectrum c is significantly different from the equilibrium spectrum (spectrum d).

Identification of Chemical Species During the Solubilization Process. The broad absorption band located at 580 nm results from the contributions of the oxidized species S_4N^- and of the reduced species S_3^-.[4] It has been found that the contribution of S_3^- to the absorbance at 580 nm is always small, especially for a relatively low temperature such as −35 °C.[4,6,7] For the sake of simplicity, it is considered that the absorbance at 580 nm is due to S_4N^-. The variations of the absorbance at 580 nm versus time as shown by Figures 1–3 suggest that S_4N^- is formed after several sequential reactions. For the study of the solubilization process at −35 °C reported in Figure 1, the difference between the equilibrium spectrum (spectrum d) and spectrum c suggests that S_4N^- is formed from a chemical species that absorbs at about 460 nm. This argument can be developed. Intermediate absorption spectra between spectrum c and spectrum d of Figure 1 are displayed in Figure 4. The differences between these spectra and spectrum c are plotted in Figure 5. It is shown in Figure 5 that the increase of S_4N^- results from the decrease of the absorbance

at 460 nm. This means that the shift of the absorption band from 450 to 420 nm (Figure 4) during the solubilization process results from the decrease of the concentration of a chemical species absorbing at 460 nm. Let us show that this is S_3N^-, a chemical species more oxidized than S_4N^-. We have previously identified S_3N^- in solutions of sulfur in liquid ammonia by Raman spectroscopy under resonance conditions.[4] Bojes et al. found that S_3N^- absorbs at 460 nm in acetonitrile,[12] and Prestel found the same result for solutions of S_3N^- in ammonia.[10] Recently we have shown that the addition of an alkali amide to a sulfur–ammonia solution makes the oxidized species more oxidized and the reduced species more reduced;[5] it was then observed that S_4N^- is gradually replaced by S_3N^-. These results led us to the interpretation of the variations displayed in Figure 5: the concentration increase of S_4N^- (Figure 5) and the absorption band shift from 450 to 420 nm (Figure 4) result from the concentration decrease of S_3N^-. The species S_3N^- is therefore an intermediate species and is a precursor species of S_4N^-. When the solubilization is monitored at −35 °C, the species S_3N^- goes through a maximum concentration (spectrum c of Figure 1). The variations displayed in Figure 5 with an isosbestic point at about 500 nm were not exactly reproduced when the solubilization process was monitored at −15 °C. This is interpreted in the following way: the reaction leading to S_4N^- from S_3N^- is faster at higher temperatures and leads to a smaller stationary concentration of S_3N^-.

The results mentioned above show that S_4N^- is produced from S_3N^-, but which species is a precursor of S_3N^-? Chivers has suggested that it may be S_2N^-.[17] This problem cannot definitely be answered from the experimental point of view. It is seen in Figure 1 that, at the beginning of the solubilization process, the absorbance increases sharply between 250 and 300 nm, the absorbance for wavelengths smaller than ca. 220 nm being assigned to NH_3. The problem of the precursor of S_3N^- could possibly be solved if the origin of the absorbance between about 250 and 450 nm could be interpreted. Let us show that S_7N^- and cyclic S_8 are not observed.

About the possible formation of S_7N^- in these solutions, as suggested by Chivers and Lau,[1] it was found that S_7N^- is fully disproportionated in liquid ammonia.[5] The absorption band of S_7NH in an inert solvent is located at 256 nm.[10] This band was observed at the very beginning of the solubilization of a sample of S_7NH in liquid ammonia, and this band broadens gradually when the disproportionation of S_7N^- takes place. Two additional arguments indicate that S_7N^- is not present in sulfur–ammonia solutions: (i) The characteristic Raman spectrum of S_7N^- is not observed,[15] even at the beginning of the solubilization process, when the solutions are not yet deeply colored. (ii) The formation process of the oxidized species S_4N^- involves more oxidized species such as S_3N^- and does not involve less oxidized species such as S_7N^-. The nonobservation of S_7N^- during the sulfur solubilization process in ammonia is rather important for the elaboration of the model of the reaction mechanism between sulfur and ammonia. The formation of S_7N^- during the solubilization of sulfur in ammonia was previously speculated by Chivers and Lau.[1]

At the beginning of the solubilization process, the absorbance increases in the UV range. This is evidenced in the absorption spectra recorded before spectrum a of Figure 1. An absorption band is then observed at ca. 300 nm, and a shoulder at 250 nm.

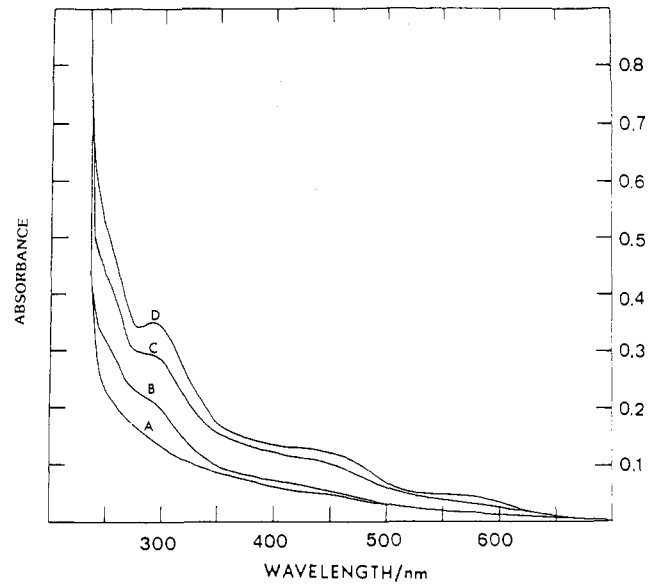

Figure 6. Absorption spectra at −35 °C during the solubilization at −35 °C of a sulfur–ammonia solution with addition of ammonium chloride (10^{-2} M): (A) spectrum of pure NH_3 at −35 °C; (B) spectrum 140 h after the beginning of the solubilization; (C) spectrum after 332 h; (D) spectrum after 508 h. The concentration of the solution after solubilization is 1.1×10^{-2} M. Optical path length = 1 mm. The absorption spectrum of this solution when the equilibrium state of this sample has been reached at room temperature could not be distinguished from the spectrum of a solution of the same concentration without ammonium chloride.

The comparison between these spectra and the absorption spectra of sulfur in methanol[13] leads to the conclusion that cyclic S_8 is not present in sulfur solutions in liquid ammonia. Furthermore, the characteristic Raman bands of cyclic S_8 at 475 and 218 cm^{-1} have never been observed.[14] These results lead to the conclusion that cyclic S_8 is not present in sulfur solutions in liquid ammonia, even during the solubilization process.

It was recently shown,[5] through the study of the influence of amide addition to the solution, that, in the equilibrium state, a fraction of the solubilized sulfur is still in the zero oxidation state and that this sulfur, different from cyclic S_8, absorbs at ca. 300 nm. This species S_{am}, absorbing at ca. 300 nm, appears first when solid sulfur is solubilized. It will be suggested in the Discussion that the solubilization of c-S_8 gives S_{am}, which is partly disproportionated. The S_{am} concentration at equilibrium will be estimated in the Discussion. Is there an intermediate species between S_{am} and the oxidized species S_3N^-? There is no experimental answer to this question, which will be also considered in the Discussion.

Influence of Amide Ions and of Ammonium Ions on the Solubilization. The influence of pH on the solubilization of sulfur in liquid ammonia has been studied via amide or ammonium addition to ammonia. This has been done to check the hypothesis of Chivers and Lau[1] that the first step of the reaction between sulfur and ammonia is the nucleophilic attack of S_8 by NH_2^-. Qualitative observations have shown that sulfur is solubilized at dry ice temperature when amide has been added to ammonia: the samples are deeply colored after 1 h, while they stay colorless when there is no amide addition. Quantitative observations have been made for the influence of ammonium addition. This is reported in Figure 6, when the solubilization is monitored at −35 °C. It is found that the ammonium additions slow down the solubilization process (Figure 2). These experiments confirm the hypothesis of Chivers and Lau.[1] The concentration of amide in ammonia results from the self-dissociation of ammonia and is very small.[16] This explains the very slow solubilization process of sulfur in ammonia, but it does not account for the high solubility observed. Consequently, we suggest that amide has a catalytic role and is regenerated via proton exchange. This will be considered in the Discussion. This does not rule out the possibility of a direct nucleophilic attack of c-S_8 by NH_3 itself. In basic and neutral solution, this process

(12) Bojes, J.; Chivers, T.; Laidlaw, W. G.; Trsic, M. *J. Am. Chem. Soc.* **1982**, *104*, 4837.
(13) (a) Meyer, B.; Gouterman, M.; Jensen, D.; Oomen, T. V.; Spitzer, K.; Stroyer-Hansen, T. In *Sulfur Research Trends*; Miller, D. J., Wiewiorowski, T. K., Eds.; Advances in Chemistry 110; American Chemical Society: Washington, DC, 1971; p 53. (b) Meyer, B.; Oomen, T. V.; Jensen, D. *J. Phys. Chem.* **1971**, *75*, 912.
(14) (a) Anderson, A.; Loh, Y. T. *Can. J. Chem.* **1969**, *47*, 879. (b) Steudel, R. *Spectrochim. Acta* **1975**, *31A*, 1065. (c) Meyer, B. *Chem. Rev.* **1976**, *76*, 367.
(15) Steudel, R. *J. Phys. Chem.* **1977**, *81*, 343.
(16) (a) Herlem, M. *Bull. Soc. Chim. Fr.* **1967**, 1687. (b) Herlem, M.; Thiebault, A. *Bull. Soc. Chim. Fr.* **1970**, 383.
(17) Chivers, T.; Laidlaw, W. G.; Oakley, R. T.; Trsic, M. *J. Am. Chem. Soc.* **1980**, *102*, 5773.
(18) Chivers, T.; Hojo, M. *Inorg. Chem.* **1984**, *23*, 2738.

Table I. Distribution of Solubilized Sulfur among the Various Chemical Species

sulfur concn C, 10^{-5} M	43	90	100	132	900
S_4N^- concn, 10^{-5} M	1.9	4.3	4.5	5.7	26
C_0,[a] 10^{-5} M	2.0	3.8	4.2	5.5	14.1
α (290 K) for $S_6^{2-} \rightleftarrows 2S_3^-$	0.979	0.959	0.955	0.947	0.882
% sulfur in S_4N^-, S_6^{2-}, S_3N^-	47	47	46	44	25
% sulfur in S_{am}	53	53	54	56	74

[a] The concentration C_0 in association with the equilibrium constant K ($\ln K = -5296/T + 12.66$) (i.e. $K = 3.6 \times 10^{-3}$ at 290 K and ΔH = 44 kJ M^{-1}) gives the calculated values of absorbance at 610 nm that best fit the experimental values (Figure 7).

would be much slower than the attack by NH_2^-. But it could take over in acidic solutions where the concentrations of NH_2^- become exceedingly small.

Concentration of S_4N^- in the Equilibrium State. The concentration of S_4N^- in sulfur–ammonia solutions in the equilibrium state will now be determined. This will show that the concentration of S_4N^- is much lower than expected from eq 1. The determination of the S_4N^- concentration only requires the molar extinction coefficient of this species, since the absorbance of S_4N^- is easily known. We have previously obtained[4] the Beer plot for the absorption band at 580 nm and 200 K when the contribution of S_3^- is negligible. When eq 1 was used, this led[4] to an apparent extinction coefficient of 7290 M^{-1} cm^{-1}, assuming that the reaction was complete. However, it has been recently shown[5] through the study of solutions of S_7NH in NH_3 that the extinction coefficient of S_4N^- in ammonia is close to the value (16 000 M^{-1} cm^{-1}) obtained by Chivers et al. in acetonitrile.[17] This value has therefore been used for the determination of the concentration of S_4N^- (Table I), and it is obvious that eq 1 overestimates the concentration of S_4N^- by a factor of about 2.

Concentration of S_6^{2-} in the Equilibrium State. Since S_6^{2-} is partly dissociated into S_3^- according to eq 2, we are interested in the total content of $[S_6^{2-}] + [S_3^-]/2$, which we call C_0.

It is presently impossible to calculate the concentration of S_6^{2-} from the absorption spectra. In sulfur solutions in ammonia the absorption band located between 460 and 420 nm contains the contribution of S_6^{2-} and S_3N^- and has not been resolved.

However, it is possible to calculate the concentration of S_3^- from the absorption at 610 nm, in spite of the strong absorption of S_4N^- at 580 nm. This estimate is made in the following way. At 200 K, S_3^- is fully associated in S_6^{2-} and the absorption in the 580–610 nm range is due to S_4N^- only. When the temperature increases, S_6^{2-} is partly dissociated, S_4N^- is not affected, and the difference between the absorptions at T and 200 K gives the absorption of S_3^- at T.

In order to calculate the concentrations of S_3^- and S_6^{2-}, we need the extinction coefficient $\epsilon(S_3^-)$ at 610 nm and the equilibrium constant K_T of eq 2. These have been obtained from the absorption spectra of Li_2S_6 in ammonia solutions and are $\epsilon(S_3^-) = 5100 \pm 300$ M^{-1} cm^{-1} and $K_T = K_0 \exp(-\Delta H/RT)$ with $K_T = 4.3 \times 10^{-3}$ at 298 K and ΔH = 48 kJ M^{-1}.[6]

However, since the solutions of Li_2S_6 are neutral while the solutions of sulfur are acidic, a doubt remained about the use of the same equilibrium constant in both cases. K_T has been therefore recalculated from the absorption spectra of S_3^- in sulfur solutions by using the equations

$$K_T = [S_3^-]^2/[S_6^{2-}] = \frac{4C_0\alpha^2}{1-\alpha} \quad (3)$$

$$A(610) = [S_3^-]d\epsilon(S_3^-) = 2C_0\alpha d\epsilon(S_3^-) \quad (4)$$

where d is the optical path length and α the dissociation coefficient of eq 2. The unknowns, at each temperature, are C_0, α, and $K_T = K_0 \exp(-\Delta H/RT)$.

A numerical analysis of this problem has shown that the best fit (Figure 7) between calculated and experimental values of $A(610)$ is obtained with $K_T = 3.6 \times 10^{-3}$ at 290 K, ΔH = 44 kJ M^{-1}, and values of C_0 and α that are reported in Table I. These values of K and ΔH are indeed very close to the values obtained with solutions of Li_2S_6.

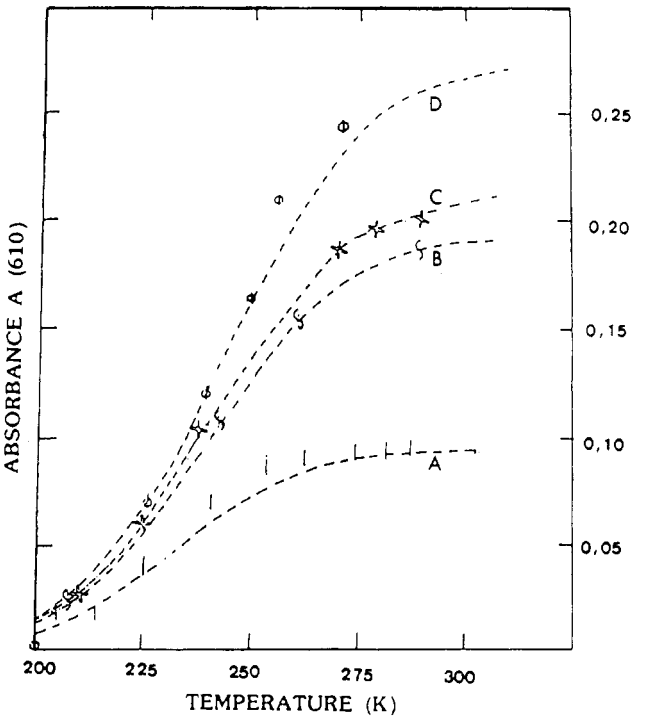

Figure 7. Variations of the absorbance of S_3^- at 610 nm versus temperature for sulfur–ammonia solutions: (A) 4.3×10^{-3} M; (B) 9×10^{-4} M; (C) 10^{-3} M; (D) 1.3×10^{-3} M. The dotted lines have been calculated with the equilibrium constant K_T ($\ln K_T = -5296/T + 12.66$) and with the values of C_0 from Table I.

Table I shows that eq 1 overestimates the concentration C_0 by approximately the same numerical factor as for S_4N^-. It indicates also that the ratios of C_0 over initial sulfur concentration slightly decrease when the concentrations increase.

Concentration of S_{am} in the Equilibrium State. It has been shown, recently, through the study of the influence of the addition of an alkali amide to the solution, that a fraction of solubilized sulfur remains in the zero oxidation state. This sulfur is noted S_{am} to indicate the possible interaction with ammonia. It was found that S_{am} absorbs around 300 nm, but our present knowledge does not allow the determination of the concentration of S_{am} from the absorbance at 300 nm. It is considered that sulfur (S_8) in liquid ammonia gives S_{am}, S_6^{2-}, S_4N^-, and S_3N^-. The concentrations of S_4N^- and S_6^{2-} have been determined above. The S_3N^- concentration can only be estimated by assuming that the extinction coefficient of S_3N^- at 460 nm has a numerical value close to that of S_4N^- at 580 nm. Furthermore, the absorbance of S_3N^- at 460 nm cannot be directly measured from the absorption spectrum of a sulfur–ammonia solution, because S_6^{2-} also absorbs in this wavelength range. It was shown above that, for the most dilute solutions, the dissociation of S_6^{2-} is high at room temperature; it is considered that, in these conditions, the absorbance at 460 nm can be assigned to S_3N^-. It follows that the concentration of S_3N^- is less than one-tenth of the concentration of S_4N^-. It is realistic to consider that this overestimation of the concentration of S_3N^- relative to that of S_4N^- is valid in the whole concentration range. It is also considered that the concentration of S_3N^- is temperature independent, as experimentally observed for S_4N^-.

The concentrations of S_6^{2-} and S_4N^- have therefore been determined, and that of S_3N^- has been estimated. The S_{am} concentration can therefore be deduced. These results are displayed in Figure 8, as the percentage of solubilized sulfur under the various species (S_6^{2-}, S_4N^-, S_3N^-, S_{am}). Figure 8 shows that S_{am} corresponds to more than 50% of solubilized sulfur. This fraction increases when the concentration of the solutions increases and is as high as 75% for ca. 10^{-2} M solutions. This means that the disproportionation of sulfur decreases when the concentration increases, as in any conventional dissociation equilibrium. This result confirms another observation: when S_{am} is transformed to

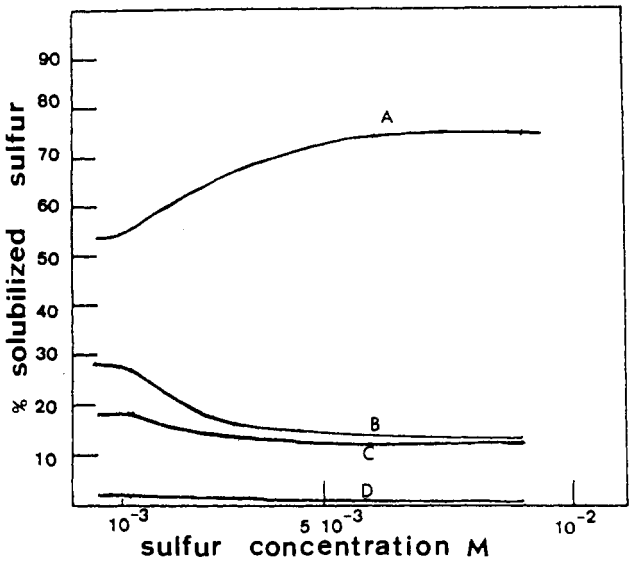

Figure 8. Percentage distribution of solubilized sulfur among the various chemical species: (A) in S_{am}; (B) in S_6^{2-}; (C) in S_4N^-; (D) in S_3N^- (estimated to 2%).

S_4N^- under amide addition, the relative increase of the concentration of S_4N^- increases with the concentration of the solution.

Discussion

Disproportionation Constant of Sulfur in Ammonia. The above analysis shows that sulfur is not fully disproportionated in liquid ammonia. We now turn to an estimation of the disproportionation constant. This requires an equation for the disproportionation equation. It was shown above that the concentration of S_3N^- is less than one-tenth of the concentration of S_4N^- and that there is approximately 1 S_4N^- for 22 solubilized atoms of sulfur, for dilute solutions. Consequently, S_3N^- corresponds to less than 2% of solubilized sulfur, and S_3N^- will be ignored in the following analysis. For the sake of simplicity, it is assumed that S_{am} corresponds to only one species, which is a chain of sulfur S_n. The disproportionation of sulfur in ammonia is then described by the equation

$$(10/n)S_n + 4NH_3 \rightleftarrows S_4N^- + 2S_3^- + 3NH_4^+ \quad (5)$$

S_3^- is chosen rather than S_6^{2-} because its concentration is determined experimentally through its absorbance. It is in equilibrium with S_6^{2-}. Equation 5 allows the definition of the disproportionation constant K_n given by

$$K_n = [S_4N^-][S_3^-]^2[NH_4^+]^3[S_n]^{-10/n} \quad (6)$$

For each value of n, K_n can be calculated. It is shown in Table II that K_n increases with concentration for $n \geq 3$ and decreases when concentration increases for $n = 1$. However, for $n = 2$, K_2 is almost concentration independent. This suggests that the zerovalent sulfur species at equilibrium involves two sulfur atoms. In the following section, S_{am} at equilibrium will be written S_{2am}, for the sake of simplicity.

The strongest evidence for S_{2am} comes from the influence of amide addition, together with the determinations of the concentrations of the various chemical species. The best experimental evidence of S_{2am} is the absorbance around 300 nm: this band appears at the beginning of the solubilization process and decreases under amide addition. There is no evidence for S_{2am} from Raman spectroscopy. The Raman experiments have been performed with excitation wavelengths in the visible range. The Raman spectra under resonance conditions could possibly be obtained by using UV excitation wavelengths. However, if the S–S vibration of S_{2am} is Raman active, the corresponding line will quite probably be located in the 400–500-cm^{-1} range together with the Raman lines of S_6^{2-}.

It is quite interesting that previous investigators have already suggested the presence of chemical species of the S_{2am} type in sulfur–ammonia solutions. Kerouanton et al. have suggested the presence of S_2NH_3 in these solutions from cryoscopic studies.[19] Sato et al. have suggested from organic syntheses using sulfur–ammonia solutions that chemical species such as H_2NS^- and H_2NSS^- should be present in the solution.[20]

Table II. Estimation of the Disproportionation Constant K_n of Sulfur in Ammonia[a]

sulfur concn, 10^{-5} M	43	90	100	132
S_3^- concn, 10^{-5} M	3.8	7.8	8.6	10.6
S_4N^- concn, 10^{-5} M	1.9	4.3	4.5	5.7
S_{am} concn, 10^{-5} M	22.7	47.7	54.0	73.9
$10^{19}K_8$	0.025	0.091	1.16	3.4
$10^{12}K_3$	0.28	2.1	2.1	3.3
$10^{7}K_2$	2.8	6.1	4.9	4.1
$10^{-10}K_1$	1.4	0.078	0.034	0.006

[a] The values of K_n have been calculated with $K_n = 27[S_4N^-]^4 \times [S_3^-]^2[S_n]^{-10/n}$.

A Model for the Mechanism of Reaction between Sulfur and Ammonia. As recalled in the Introduction, a model for the mechanism of reaction between sulfur and ammonia has first been suggested by Chivers and Lau.[1] Our results confirm their hypothesis that the amide ion NH_2^- has a key role in the first step of the mechanism but discard the possible formation of S_7N^- during the solubilization process. Our results show that S_4N^- is formed from the precursor species S_3N^-. These results are used to propose an improved model of the mechanism of reaction between sulfur and ammonia.

The first step of the reaction mechanism is the opening of cyclic S_8 by nucleophilic attack of NH_2^-:

$$c\text{-}S_8 + NH_2^- \rightarrow S_8NH_2^- \quad (7)$$

However, the small concentration of amide in ammonia does not explain the high solubility of sulfur in ammonia. It is therefore assumed that amide is regenerated by proton exchange:

$$S_8NH_2^- + NH_3 \rightleftarrows S_8NH_3 + NH_2^- \quad (8)$$

The species S_8NH_3 can be written

$$^-S\text{–}S\cdots S\text{–}N^+H_3$$

and this explains its solubility. Furthermore, other S–S bonds in this molecule can undergo the same nucleophilic attack and yield smaller S_xNH_3 molecules such as S_2NH_3 according to

$$S_8NH_3 + 3NH_3 \rightarrow 4S_2NH_3 \quad (9)$$

Meanwhile the same S_8NH_3 undergoes a disproportionation. In order to write its successive steps, let us recall that (i) the Raman spectra recorded during the solubilization process have displayed the bands assigned to S_6^{2-} and (ii) there was no experimental indication of the presence of S_7N^- at equilibrium and during the solubilization process and it was observed that S_4N^- is formed through S_3N^-. Since S_3N^- cannot be produced directly from S_8NH_3 with S_6^{2-}, it is assumed that it originates from S_2N^-. The disproportionation of S_8NH_3 may then be written

$$S_8NH_3 \rightarrow S_6^{2-} + S_2NH_3^{2+} \quad (10)$$

$$S_2NH_3^{2+} + 3NH_3 \rightarrow S_2N^- + 3NH_4^+ \quad (11)$$

The species S_2N^- produced by eq 11 is asymmetric with both S atoms on the same side of the N atom (S–S–N^-) and is different from the known symmetric species (S–N–S^-).[12,18] It is unstable and can lead to S_3N^- and S_4N^- through reactions with S_2NH_3 resulting from eq 9:

$$S_2N^- + S_2NH_3 \rightarrow S_3N^- + SNH_3 \quad (12)$$

$$S_3N^- + S_2NH_3 \rightarrow S_4N^- + SNH_3 \quad (13)$$

$$2SNH_3 \rightarrow S_2NH_3 + NH_3 \quad (14)$$

Equations 9–14 give the expression of the equilibrium, by elim-

(19) Kerouanton, A.; Herlem, M.; Thiebault, A. *Anal. Lett.* **1973**, *6*, 171.
(20) Sato, R.; Sato, T.; Segawa, K.; Takikawa, Y.; Takizawa, S.; Oae, S. *Phosphorus Sulfur* **1979**, *7*, 217.

ination of the unstable species:

$$5S_2NH_3 \rightleftarrows S_6^{2-} + S_4N^- + 3NH_4^+ + NH_3 \quad (15)$$

or

$$9S_2NH_3 \rightleftarrows 2S_6^{2-} + 2S_3N^- + 6NH_4^+ + NH_3 \quad (15')$$

These equilibria are complex but may be reached through a small number of simple steps. This model for the solubilization process takes into account the nonobservation of S_7N^-. It should be noted that the formation of S_4N^- from S_2N^- considered as intermediate species has already been suggested by Chivers et al.[17] The present model takes into account our observation that S_3N^- is the precursor species of S_4N^-. Consequently, it has been assumed that S_2N^- is the precursor species of S_3N^-.

Conclusion

The experimental results reported in the present paper give a new insight into the process of formation of chemical species in the solutions of sulfur in liquid ammonia and lead unambiguously to the description of the equilibrium state. A model is proposed for the reaction mechanism between c-S_8 and liquid ammonia, which also explains the formation process of sulfur–nitrogen species such as S_4N^- and S_3N^- in liquid ammonia. It must be noted that the heptasulfur imido anion S_7N^- is not involved in this mechanism. Two points are somewhat speculative: S_2NH_3 is the zerovalent sulfur species at equilibrium, but this species has already been suggested by other investigators; our analysis of the disproportionation constant supports this point. The other speculative point is that S_2N^- could be the precursor species of S_3N^-.

It is shown that the disproportionation of sulfur in ammonia leads to an equilibrium. The quantitative determination of the amount of solubilized sulfur that remains in the zero state of oxidation (S_{am}) is given.

Acknowledgment. This research was suported by the CNRS (ATP Application de l'électricité à la chimie No. 249) and by the AFME (décision d'aide à la Recherche No. 4213 9261). We acknowledge a reviewer for mentioning the relevance of ref 19 and 20 to the present work.

Registry No. S, 7704-34-9; NH_3, 7664-41-7; NH_4Cl, 12125-02-9.

Contribution from the Department of Chemistry and Biochemistry, Texas Tech University, Lubbock, Texas 79409-1061

Some Perfluoroalkyl-Substituted Tripnicogens and Their Hydrolysis To Yield Chiral Dipnicogens[1]

Larry R. Avens,† Richard A. Wolcott, Leonard V. Cribbs, and Jerry L. Mills*

Received July 30, 1987

The insertion of a perfluoroalkylphosphinidene moiety R_f from perfluoroalkylcyclopolyphosphines $(R_fP)_n$ into the pnicogen–pnicogen bond of tetraalkyldipnicogens appears to be general. Thus a CF_3P unit from $(CF_3P)_{4,5}$ reacts either with R_2PPR_2 (where R = Me, Et, Bu) or with $Me_2AsAsMe_2$ to form the tripnicogen compounds $R_2PP(CF_3)PR_2$ and $Me_2AsP(CF_3)AsMe_2$, respectively. Similarly $(C_2F_5P)_{3,4}$ reacts with Me_2PPMe_2 to form $Me_2PP(C_2F_5)PMe_2$. Any two symmetric tripnicogens, such as $Me_2PP(CF_3)PMe_2$ and $Et_2PP(CF_3)PEt_2$, undergo a scrambling reaction to form an equilibrium mixture containing the asymmetric tripnicogen. The tripnicogens undergo neutral water hydrolysis surprisingly easily to form chiral dipnicogens. For example, $Me_2PP(CF_3)PMe_2$ hydrolyzes immediately at ambient temperature with an equimolar quantity of water to yield the new chiral secondary phosphine $Me_2PP(CF_3)H$ plus $Me_2P(O)OH$ and Me_2PH. Similarly, hydrolysis of the appropriate tripnicogen yields the chiral dipnicogen secondary phosphines $Me_2PP(C_2F_5)H$, $Et_2PP(CF_3)H$, $Bu_2PP(CF_3)H$, and $Me_2AsP(CF_3)H$. A second equivalent of water hydrolyzes the dipnicogens to the primary perfluoroalkylphosphine. Possible reaction mechanisms are discussed together with NMR data.

Introduction

The RP moiety in a cyclopolyphosphine $(RP)_n$ is isoelectronic with sulfur. Burg synthesized the phosphinidene complex $Me_3P{\rightarrow}P(CF_3)$ from the reaction of Me_3P with $(CF_3P)_{4,5}$, analogous to the formation of $Me_3P{=}S$.[2] Cowley and Dierdorf observed that the reaction of Me_2PPMe_2 with $(CF_3P)_{4,5}$ yields neither the mono- nor the diphosphinidene complex, but rather the insertion product $Me_2PP(CF_3)PMe_2$.[3] We observed that the phosphorus–phosphorus bond in the triphosphine $Me_2PP(CF_3)PMe_2$ is surprisingly easily hydrolyzed by neutral water at ambient temperature to quantitatively yield the new chiral diphosphine $Me_2PP(CF_3)H$.[4] Because of the potentially interesting chemistry of this type of chiral diphosphine relative to addition to alkenes, alkynes, or metal–metal bonds, we have examined the generality of the insertion reaction of perfluoroalkylphosphinidenes and the subsequent hydrolysis to the tripnicogens to yield chiral dipnicogens. These chiral disphosphines may also be of interest because of the catalytic properties of chiral phosphines in asymmetric syntheses. Perfluoroalkyl-substituted polyphosphines are of current general interest.[5]

Results

Insertion of Perfluoroalkylphosphinidene into the Pnicogen–Pnicogen Bond of Diphosphines and Diarsines. As reported by Cowley and Dierdorf, the reaction of equimolar amounts[6] of tetramethyldiphosphine Me_2PPMe_2 with $(CF_3P)_{4,5}$ quantitatively

† Present address: MS E501, Los Alamos National Laboratory, Los Alamos, NM 87545.

(1) Pnicogens refer to main group V compounds. Therefore, for example, dipnicogen simply refers to a compound containing two main group V elements such as a diphosphine or arsinophosphine. Suchow, L. *Inorg. Chem.* **1978**, *17*, 2041.
(2) (a) Burg, A. B.; Mahler, W. *J. Am. Chem. Soc.* **1961**, *83*, 2388. (b) Burg, A. B. *J. Inorg. Nucl. Chem.* **1971**, *33*, 1575.
(3) (a) Cowley, A. H.; Dierdorf, D. S. *J. Am. Chem. Soc.* **1969**, *91*, 6609. (b) Cowley, A. H. *J. Am. Chem. Soc.* **1967**, *89*, 5990.
(4) Presented in part at the Second International Conference on Phosphorus Chemistry, Durham, NC, June, 1981.
(5) Burg, A. B. *Inorg. Chem.* **1986**, *25*, 4751. Burg, A. B. *Inorg. Chem.* **1985**, *24*, 3342. Burg, A. B. *Inorg. Chem.* **1985**, *24*, 2573. Burg, A. B. *Inorg. Chem.* **1981**, *20*, 3731. Burg, A. B. *Inorg. Chem.* **1981**, *20*, 3734. Grobe, J.; Haubold, R. *Z. Anorg. Allg. Chem.* **1986**, *534*, 121. Grobe, J.; Le Van, D.; Schulze, L. *Z. Naturforsch.* **1985**, *40B*, 1753. Steger, B.; Oberhammer, H.; Grobe, J.; Le Van, D. *Inorg. Chem.* **1986**, *25*, 3177. Khokhryakov, K. A.; Maslennikov, I. G.; Grigorov, E. I.; Kukushkin, Yu., N. *Zh. Obshch. Khim.* **1985**, *55*, 2622. Maslennikov, I. G.; Lyubimova, M. V.; Krutikov, V. I.; Lavrent'ev, A. N. *Zh. Obshch. Khim.* **1983**, *53*, 2646 and references therein.
(6) Equimolar quantities of $(R_fP)_n$ means equimolar quantities of R_fP units.

0020-1669/89/1328-0200$01.50/0